Journal of JSEM, Vol.12, Special Issue (2012) s232-s236


# Filtration of Ni-Al Alloy Containing By-Product Alumina in Centrifugal Combustion Synthesis

Tatsuya OHMI[1] and Manabu IGUCHI[1]

[1] Faculty of Engineering, Hokkaido University, Sapporo, Hokkaido, 060-8628, Japan

(*Received 10 December 2011; received in revised form 14 March 2012; accepted 26 April 2012*)

**Abstract**

The centrifugal combustion synthesis (CCS) process with a thermite-type combustion synthesis reaction can produce a joint of a cast $Ni_3Al$ member and a dissimilar material. We verify effectiveness of filtration of the combustion-synthesized Ni-Al alloy on the distribution of by-product alumina inclusions in the cast member. In the specimen produced without filtration, coarse alumina inclusions were distributed. In contrast, no such a fatal defect was observed in the filtrated specimen.

**Key words**

Centrifugal Combustion Synthesis, Centrifugal Casting, Thermite Combustion Synthesis Reaction, Nickel Aluminide, Filtration, Alumina Inclusion, Centrifugal Separation

## 1. Introduction

Some intermetallic compounds, including aluminides of nickel or iron, have widely been studied for high-temperature structural use because of their attractive properties such as low density, high hardness, good oxidation resistance, and excellent strength at elevated temperatures. However, these intermetallic compounds often have low tensile ductility and exhibit brittle fracture. [1-2] Combination with a ductile material is one of the promising ways to use them.

One of the authors previously proposed a centrifugal combustion synthesis (CCS) process to produce a joint of an intermetallic compound and a dissimilar material, for example, a joint of tri-nickel aluminide ($Ni_3Al$) and steel. [3] In the CCS process, high-temperature liquid of the intermetallic compound is produced by combustion synthesis and the product is simultaneously cast and welded on the base of the dissimilar material. Molten $Ni_3Al$ can be produced by a thermite combustion synthesis reaction from Ni, NiO and Al powders. NiO is used to control the heat evolution in the reaction. However, such a reaction also produces alumina ($Al_2O_3$) as the by-product which may form coarse inclusions and harm the mechanical properties of the cast $Ni_3Al$. The by-product $Al_2O_3$ must be separated from the molten alloy. This problem becomes serious especially when the configuration of the mold cavity is complicated and thus centrifugal separation of the $Al_2O_3$ inclusions [3] is not effective. In such a case, the inclusions must be filtered before casting. From above standpoint, this study investigated the effect of filtration of the combustion-synthesized molten alloy on the distribution of the $Al_2O_3$ inclusions in the cast $Ni_3Al$ member. We also investigated the floating behavior of the $Al_2O_3$ inclusions in molten Ni-Al alloys under a centrifugal force field as an introductory study.

## 2. Experimental Procedure

### 2.1 Thermite combustion synthesis reaction

In order to produce the molten $Ni_3Al$ alloy, we adopted a thermite combustion synthesis reaction [4, 5], Eq. (3), which combines the ordinary combustion synthesis reaction, Eq. (1), and a modified thermite reaction, Eq. (2).

$$3Ni + Al = Ni_3Al \quad (1)$$

$$3NiO + 3Al = Ni_3Al + Al_2O_3 \quad (2)$$

$$3a_TNiO + 3(1-a_T)Ni + (1+2a_T)Al = Ni_3Al + a_TAl_2O_3 \quad (3)$$

In Eq. (3), the coefficient $a_T$ is the ratio of the modified thermite reaction to the thermite combustion synthesis reaction. Equation (2) evolves 3.6 times more heat per unit mole total product than Eq. (1). Molten $Ni_3Al$ can thus be produced when the thermite combustion synthesis is used with an adequate value of $a_T$. The value of $a_T$ was set at 0.25 for $Ni_3Al$ synthesis.

The starting materials for the thermite combustion synthesis reaction were aluminum powder 99.5 mass% in purity and 100 μm in particle diameter, nickel powder of 99.8 mass% and 5 μm, and nickel oxide powder 97.0 mass% and 5 μm. The powder mixture was cold-pressed into a cylindrical green compact in a metal mold under a unidirectional pressure of 470 MPa. The green compact had a diameter of 20 mm, mass of 30 g, and relative density of 80 %.

### 2.2 Centrifugal casting of disk-shaped members

Figure 1(a) presents a schematic of the main rotational part of the vertical centrifugal caster used in the filtration experiments. A graphite mold with a disk-shaped cavity and a cylindrical runner; a ceramic filter; and a green powder compact of reactants consisting of Al, Ni and NiO were set in the centrifugal caster. The mold cavity was 15 mm in diameter and 2 mm in thickness. The runner was 5 mm in diameter and 10 mm in length.

The reaction was induced by heating the green powder compact in the centrifugal force field. The synthesized molten alloy flowed through the filter and then into the mold. Three kinds of filters were examined: two kinds of ceramic foams with different cell sizes and a bundle of straight ceramic pipes. The length of the filters was 20 mm. The cell size of the ceramic foam was 2.5 or 4.2 mm, which was measured by the linear intercept method. The third filter had 54 straight holes 0.8 mm in diameter. These filters consisted mainly of $Al_2O_3$.

The angular velocity of the apparatus, $\omega$, was 38π rad/s, which produced a centrifugal acceleration 85 times higher than the gravitational acceleration, $G$, at the bottom of the mold cavity. After processing, distributions of the $Al_2O_3$ inclusions on the vertical section of the cast specimens were examined.

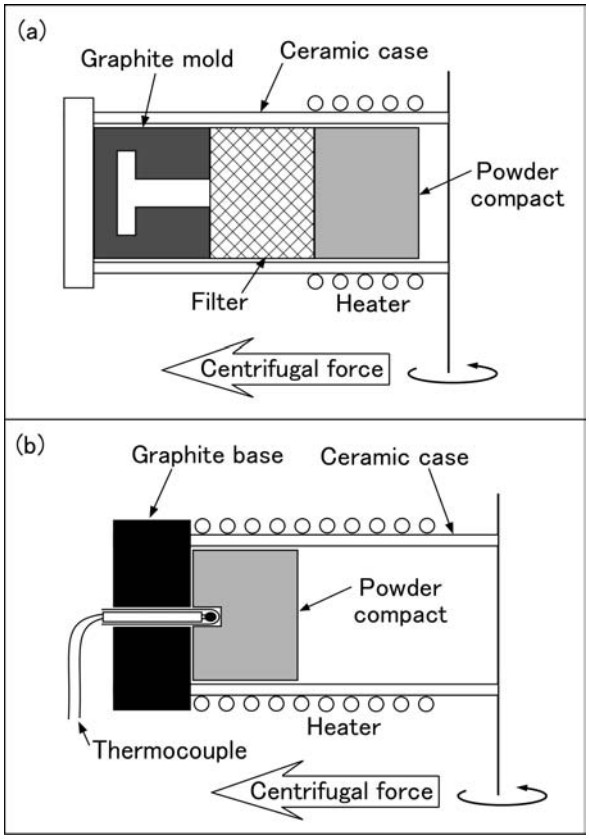


Fig .1 Schematic of apparatus. (a) Main rotational part used for the filtration experiments. (b) Apparatus for investigating the floating behavior of the $Al_2O_3$ inclusions

### 2.3 Centrifugal separation of $Al_2O_3$ inclusions

Figure 1(b) illustrates the apparatus for the introductory study to investigate the floating behavior of the $Al_2O_3$ inclusions. The green compact was set in an $Al_2O_3$-based ceramic case with a graphite base. The ceramic case had a closed porous structure which provided good thermal insulation and thermal shock resistance. Thus, the synthesized molten alloy was unidirectionally solidified on the spot. We used the following reaction with $a_T$ of 0.43.

$$a_T\mathrm{NiO} + (1-a_T)\mathrm{Ni} + (1+2a_T/3)\mathrm{Al} = \mathrm{NiAl} + (a_T/3)\mathrm{Al_2O_3} \quad (4)$$

NiAl solidifies with a planar or cellular manner. Therefore, we could consider that a macroscopically-straight solid-liquid interface moved from the bottom to the surface of the molten alloy. The centrifugal acceleration was 40*G* at the bottom.

## 3. Results

### 3.1 Floating behavior of the $Al_2O_3$ inclusions

Figure 2(a) provides a dark-field image of a vertical section of the NiAl ingot combustion-synthesized and solidified in the centrifugal force field. The longitudinal grain boundaries appearing like bright streaks in the photograph indicate almost unidirectional solidification. Figure 2(b) shows a microstructure (a back-scattered electron image) near the center of the ingot. Spherical $Al_2O_3$ particles with 6 μm or smaller diameter were observed. Although most part of by-product $Al_2O_3$ floated to the surface and formed 2 mm-thick layer, small amount of $Al_2O_3$ remained in the ingot as seen in this picture. Furthermore, the shape of the $Al_2O_3$ particles indicates that $Al_2O_3$ transiently melted just after combustion synthesis.

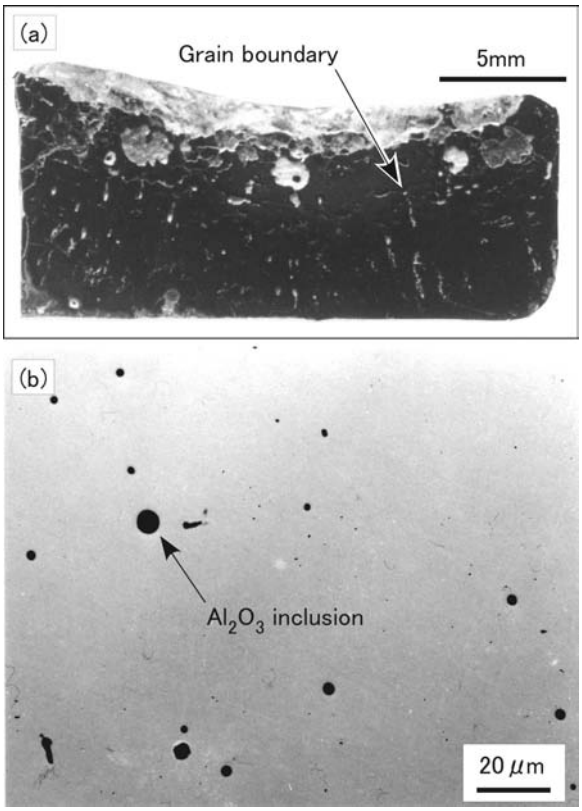


Fig. 2 Structures of the NiAl ingot combustion-synthesized and solidified in the centrifugal force field. (a) Macrostructure of the vertical section of the ingot. (b) Microstructure near the center of the ingot

Figure 3 depicts a schematic illustration of a spherical $Al_2O_3$ particle with radius *R* floating in the NiAl melt from the bottom ($r=r_0$) to the surface ($r=r_0-\Delta r_0$), where *r* is the distance from the rotation axis. The balance between the buoyancy force and the drag force on the particle is expressed by the following equation:

$$(4/3)\pi R^3(\rho_A-\rho_L)\omega^2 r = 6\pi\mu R(\mathrm{d}r/\mathrm{d}t) \quad (5)$$

where $\rho_A$ and $\rho_L$ are the densities of solid $Al_2O_3$ and liquid NiAl, respectively; and $\mu$ is the viscosity of liquid NiAl. We obtain Eq. (6) by solving Eq. (5).

$$r=r_0\exp(s\omega^2 t) \quad (6)$$

where *s* is the sedimentation coefficient expressed by the following equation.

$$s=2R^2(\rho_A-\rho_L)/9\mu \quad (7)$$

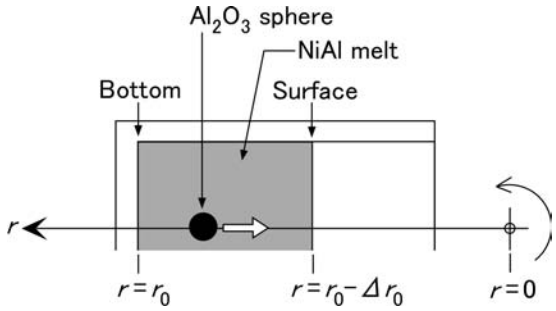


Fig. 3 Schematic illustration of a spherical $Al_2O_3$ particle floating in a NiAl melt

Table 1 Physical properties of liquid NiAl, liquid $Ni_3Al$ and solid $Al_2O_3$. [6-9]

| | NiAl (L) | $Ni_3Al$ (L) | $Al_2O_3$ (S) |
|---|---|---|---|
| Density, $\rho$ /kg m$^{-3}$ | 5900 [6] | 6810 [7] | 3970 [7] |
| Viscosity, $\mu$ /mPa s | 8.5 [8] | 5 [9] | – |

Figure 4 shows the floating behavior of the particle calculated by Eq. (6) with the physical properties listed in Table 1. This figure also shows the movement of the solid-liquid interface, which was obtained from the cooling curve assuming a constant solidification rate. All the calculation conditions corresponded to the experiment shown in Fig. 2. These results indicate that a particle 8 μm or smaller in radius can be trapped by the solidification front. Figure 4 also indicates that a 6-μm-radius or smaller particle can be trapped at the center of the ingot ($r$=23 mm). This result is consistent with the microstructure observation in Fig. 2(b).

The absolute value of the sedimentation coefficient in the case of $Ni_3Al$ is 2.5 times larger than the case of NiAl. Therefore, the $Al_2O_3$ inclusions would float faster in $Ni_3Al$.

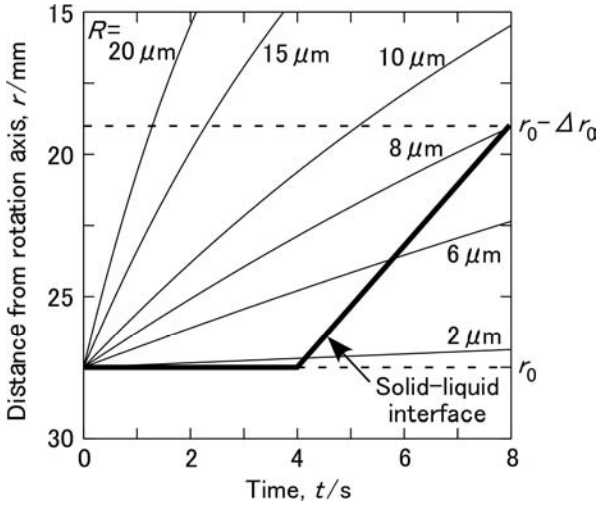


Fig. 4 Floating behavior of the $Al_2O_3$ particle and the movement of the solid-liquid interface of NiAl in the case of Fig. 2

### 3.2 Effect of filtration on the distribution of the $Al_2O_3$ inclusions

Figure 5 presents results of a centrifugal casting experiment with filtration of combustion-synthesized alloy. Figure 5(a) depicts an external appearance of the disk specimen with the runner part. Figure 5(b) shows a vertical section of the filter part after filtration. The filter successfully blocked the inflow of the large $Al_2O_3$ clump.

Figures 6(a)-(d) compare the microstructures near the peripheral part of the disk specimens produced with and without filtration. As seen in Fig. 6(a), coarse $Al_2O_3$ inclusions were trapped in the disk part. In contrast, no such a fatal defect was observed in the filtrated specimens shown in Figs. 6(b)-(d).

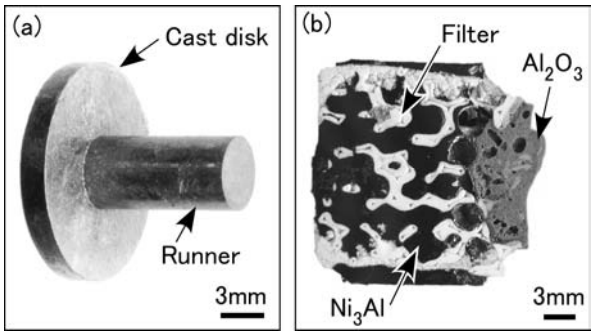


Fig. 5 Results of a centrifugal casting experiment with filtration of combustion-synthesized alloy. (a) External appearance of the cast specimen. (b) Vertical section of the ceramic filter after filtration. The cell size of the filter was 4.2 mm

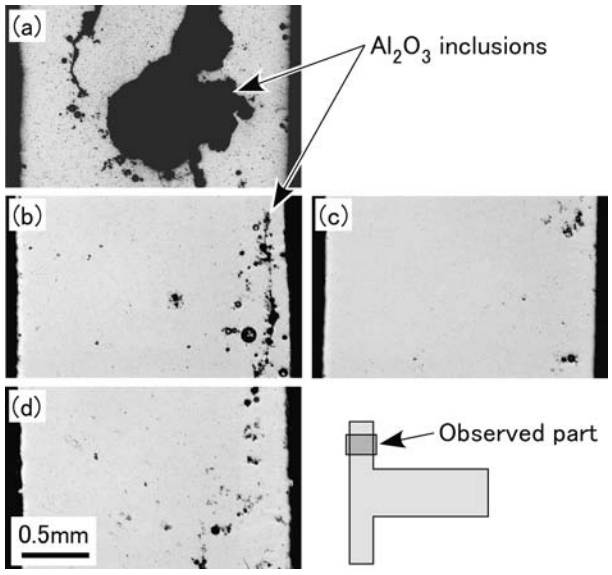


Fig. 6 Macrostructures of the cast disk. (a) No filter. (b) Filter 1: ceramic foam filter (4.2 mm in cell size). (c) Filter 2: ceramic foam filter (2.5 mm in cell size). (d) Filter 3: ceramic filter with straight holes

Figure 7 illustrates the profiles of the area fraction of the $Al_2O_3$ inclusions measured along a radius vector on a vertical section of the disk specimens. In most cases, larger amount of $Al_2O_3$ inclusions were distributed near the peripheral part of the disk.

Figure 8 presents the effect of filtration on the density of the cast specimen. This result shows that the density of the specimen was drastically changed by the presence or absence of the filter. It also shows that the ceramic foam with fine cells or the bundle of straight ceramic pipes had a good result. It is noted that the relative density of the specimen was 98.4% even in the case of the latter filter. Optimization of the structure and material of the filter is the future challenge.

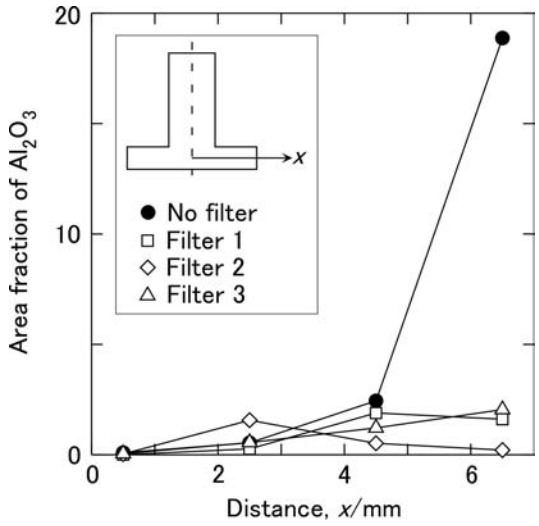


Fig. 7 Profiles of the area fractions of the $Al_2O_3$ inclusions measured on the vertical section of the cast disks

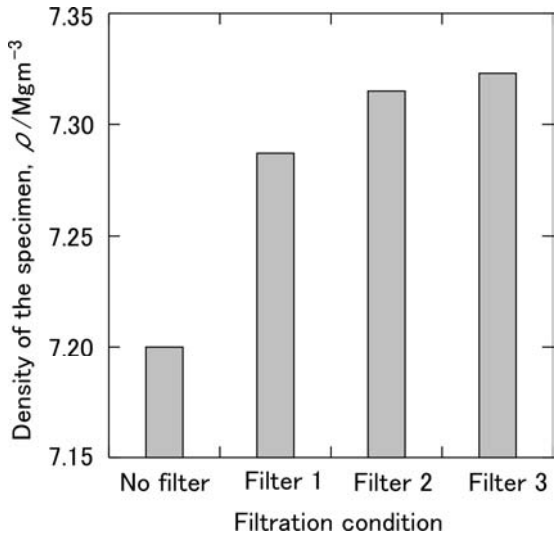


Fig. 8 Effect of filtration on the density of the cast disk

**3.3 Case example of filtration for the CCS process**

Figure 9 shows the effect of filtration on the soundness of a CCS specimen, which is a joint of a stainless-steel pipe and a cast $Ni_3Al$ pipe with an external thread [10]. Figure 9(a) illustrates the setup of the mold used for producing this CCS specimen. A simple graphite filter was used for filtration. Figures 9(b) and (c) compare the structures of the cast part of the specimens produced with and without filtration. These results demonstrate the notable effect of filtration on the soundness of the CCS specimen. In this experiment, we selected graphite as the filter material because the thickness of the filter was constrained by the size of the experimental apparatus. We also expected the graphite filter to conduct heat away from the combustion synthesized product and facilitate the solidification and agglomeration of $Al_2O_3$. However, the detailed verification of the effect of the thermal property of the filter material remains to be seen.

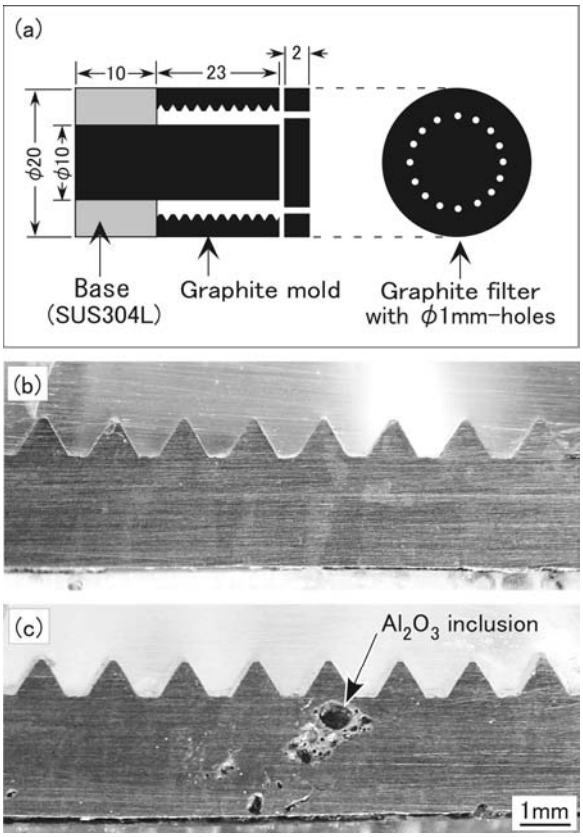


Fig. 9 Effect of filtration on the soundness of a joint of a stainless-steel pipe and a cast $Ni_3Al$ pipe with an external thread. (a) Setup of the mold. (b) Structure of the cast pipe with filtration [10]. (c) Structure of the cast pipe without filtration

**4. Conclusions**

We examined filtration of combustion-synthesized $Ni_3Al$ containing by-product $Al_2O_3$. We also investigated the floating behavior of the $Al_2O_3$ inclusions in liquid NiAl in

a centrifugal force field. The results of our investigation are summarized as follows.

(1) The floating-behavior analysis is usable for predicting the influence of the centrifugal force on the distribution of the $Al_2O_3$ inclusions trapped in the cylindrical ingot.

(2) Filtration of the combustion-synthesized alloy prevents coarse $Al_2O_3$ clumps from entering the mold cavity.

(3) The structure of the ceramic filter markedly influences the performance of the filter.

**Acknowledgement**

We would like to express our appreciation to Mr. Yasuhiro Murota and Mr. Kazuhiko Kirihara (formerly graduate students of Hokkaido University) for their assistance in the experiments.

**References**

[1] Deevi, S.C., Sikkat, V.K. and Liul, C.T.: Processing, Properties, and Applications of Nickel and Iron Aluminides, *Progress in Materials Science*, **42** (1991), 177-192.

[2] Liu, C.T., George, E.P., Maziasz, P.J. and Schneibel, J.H.: Recent advances in B2 iron aluminide alloys: deformation, fracture and alloy design, *Materials Science and Engineering*, **A258** (1998), 84-98.

[3] Ohmi, T., Kirihara, K. and Kudoh, M.: Precision Casting of Ni-Al Alloy and Simultaneous Joining to Dissimilar Metals by Modified Centrifugal Combustion Synthesis, *Mater. Trans.*, **42** (2001), 298-302.

[4] Yamada, O. and Miyamoto, Y.: Fabrication of Intermetallic Compounds by Advanced Thermite Type Combustion Synthesis Process (in Japanese), *J. Japan Inst. Metals*, **56** (1992), 938-942.

[5] Yamada, O. and Matsumoto, H.: Thermite Type Combustion Synthesis and Direct Casting of Intermetallic Compounds and Super Alloys (in Japanese), *J. Japan Foundry Soc.*, **67** (1995), 708-715.

[6] Matsuura, K., Ohsasa, K., Sueoka, N. and Kudoh, M.: In-situ Joining of Nickel Monoaluminide to Iron by Reactive Sintering, *ISIJ International*, **38** (1998), 310-315.

[7] Liu, H., Rangel, R.H. and Lavernia, E.J.: Modeling of Reactive Atomization and Deposition Processing of $Ni_3A1$, *Acta Metall, Mater.*, **42** (1994), 3277-3289.

[8] Battezzati, L. and Greer, A.L.: The Viscosity of Liquid Metals and Alloys, *Acta Metall.*, **37** (1989), 1791-1802.

[9] Sen, S., Dhindaw, B.K. and Stefanescu, D.M.: Evaluation of interface stability and melt-processing techniques of $Ni_3A1$/SiC particulate composites, *Materials Science and Engineering*, **A174** (1994), 207-216.

[10] Ohmi, T., Matsuura, K. and Kudoh, M.: Cermet/Intermetallic Joining by Centrifugal Combustion Synthesis, *International Journal of Self-Propagating High-Temperature Synthesis*, **13** (2004), 137-146.